SPT

NASA CR-134711

THE USE OF THE ION PROBE MASS SPECTROMETER IN THE MEASUREMENT OF HYDROGEN CONCENTRATION GRADIENTS IN MONEL K 500

by J.J. Truhan, Jr. and R.F. Hehemann

CASE WESTERN RESERVE UNIVERSITY

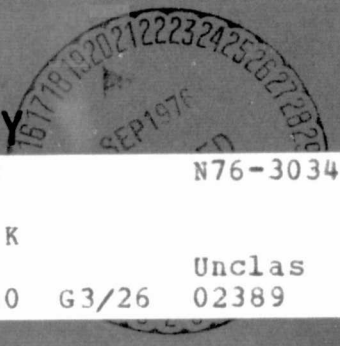

prepared for

NATIONAL AERONAUTICS AND SPACE ADMINISTRATION
NASA Lewis Research Center

GRANT NGR 36-027-051

October, 1974

NASA CR-134711

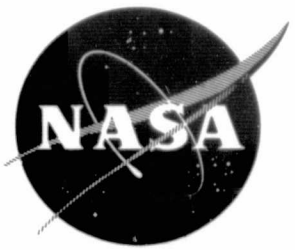

THE USE OF THE ION PROBE MASS SPECTROMETER IN THE MEASUREMENT OF HYDROGEN CONCENTRATION GRADIENTS IN MONEL K 500

by J. J. Truhan, Jr. and R. F. Hehemann

CASE WESTERN RESERVE UNIVERSITY

prepared for

NATIONAL AERONAUTICS AND SPACE ADMINISTRATION
NASA Lewis Research Center

GRANT NGR 36-027-051

October, 1974

1. Report No.	2. Government Accession No.	3. Recipient's Catalog No.
NASA CR-134711		

4. Title and Subtitle	5. Report Date
The Use of the Ion Probe Mass Spectrometer in the Measurement of Hydrogen Concentration Gradients in Monel K 500	6. Performing Organization Code
7. Author(s)	8. Performing Organization Report No.
J. J. Truhan, Jr. and R. F. Hehemann	10. Work Unit No.
9. Performing Organization Name and Address	11. Contract or Grant No.
Case Western Reserve University Cleveland, Ohio 44106	NGR 36-027-051
	13. Type of Report and Period Covered
12. Sponsoring Agency Name and Address	Summary Report 4/73-10/74
National Aeronautics and Space Administration Washington, D. C. 20546	14. Sponsoring Agency Code

15. Supplementary Notes

Project Managers, Charles W. Andrews and Hugh R. Gray
Materials and Structures Division
NASA, Lewis Research Center, Cleveland, Ohio 44135

16. Abstract

The ion probe mass spectrometer was used to measure hydrogen concentration gradients in cathodically charged Monel K 500. Initial work with the ion probe involved the calibration of the instrument and the establishment of a suitable experimental procedure for this application. Samples of Monel K 500 were cathodically charged in a weak sulfuric acid solution. By varying the current density, different levels of hydrogen were introduced into the samples. Hydrogen concentration gradients were taken by ion sputtering on the surface of these samples and monitoring the behavior of the hydrogen mass peak as a function of time. An attempt was made to determine the relative amounts of hydrogen in the bulk and grain boundaries by analyzing a fresh fracture surface with a higher proportion of grain boundary area. It was found that substantially more hydrogen was detected in the grain boundaries than in the bulk, confirming the predictions of previous workers. A sputter rate determination was made in order to establish the rate of erosion. While the gradients measured followed qualitative predictions, no effort was made to quantitatively determine hydrogen concentrations due to a lack of suitable standards.

17. Key Words (Suggested by Author(s))	18. Distribution Statement
Hydrogen Embrittlement Hydrogen Concentration Gradients Hydrogen Analyses Ion Probe Mass Spectrometer Nickel Superalloy Monel K 500	Unclassified - unlimited

19. Security Classif. (of this report)	20. Security Classif. (of this page)	21. No. of Pages	22. Price*
Unclassified	Unclassified	49	$4.25

* For sale by the National Technical Information Service, Springfield, Virginia 22151

ACKNOWLEDGEMENTS

The author wishes to thank the National Aeronautics and Space Administration and Lewis Research Center for funding this project and for providing all possible assistance.

Most grateful appreciation is expressed to Dr. R. F. Hehemann and Dr. C. W. Andrews as thesis and project advisors for their patience, aid, and encouragement during this project. Special thanks also go to Dr. H. Gray, Dr. R. F. Herzog, and Bruno Buzek for help above and beyond the call of duty.

The author wishes to kindly thank Stacy Koutsounaris for typing the manuscript.

Words are not adequate to express the loving appreciation the author feels for his parents, family, and friends without whom this thesis would be impossible.

TABLE OF CONTENTS

LIST OF TABLES

TABLE

LIST OF FIGURES

FIGURE

HYDROGEN EMBRITTLEMENT OF NICKEL-BASE ALLOYS

Hydrogen, when absorbed into a metallic system, regardless of the mode of introduction, can interact with that system in one of two basic ways (1):

a) Endothermic reaction in which hydrogen in excess of the solubility limit remains in solution or precipitates as molecular hydrogen. This type of reaction occurs in iron and steels.

b) Exothermic reaction in which a brittle hydride phase is formed by excess hydrogen such as is the case with titanium and its alloys.

Because of the variety of ways in which hydrogen can react in an alloy system, not only with the base metal, but also with the various alloy components, no unified theory of hydrogen embrittlement has been universally accepted. Two of the more popular theories will be briefly described here.

Troiano (2) has proposed that atomic hydrogen diffuses in a stress gradient to the point of maximum triaxiality at the tip of an advancing crack. This reduces the binding energy of the matrix resulting in brittle delayed failure or reduced ductility. Transition metals have been found to be most susceptible to embrittlement by hydrogen due to the added electrons from the hydrogen entering the incomplete d bands. The added electrons presumably increase

the repulsive forces which, in turn, lead to a decrease in the strength.

The pressure theory was originally proposed by Zapffe (3) and subsequently modified by Tetelman (4). In this case, it is thought that hydrogen diffuses to cracks and voids where it recombines into a gaseous form. The pressure buildup is then considered to be sufficient to promote crack propagation and decrease the ductility of the matrix.

Several basic characteristics of hydrogen embrittlement are listed (1).

a) The ductility of the metal or alloy is reduced.

b) The phenomenon is a reversible one. That is, after a suitable high temperature outgassing treatment, the original ductility is restored.

c) Slow strain rates promote embrittlement. This stems from the fact that it is necessary to allow for sufficient time for the hydrogen to diffuse to the advancing crack tip.

d) Failure will occur under a static load depending on the time and load. However, there is a lower critical stress below which failure will not occur. This lower critical stress increases as the strength is reduced.

e) The mode of fracture changes from ductile to brittle.

While the embrittling behavior of hydrogen on the ferrous alloys has been known and studied for a number of years (2), it was

generally thought that the face-centered cubic alloys were immune. More recently, however, it has been demonstrated that hydrogen embrittlement occurs in aluminum alloys (5) and austenitic stainless steels (6). Nickel has been embrittled as a result of thermal (7) and cathodic charging (8). Mihelic (9,10) and Papp (11,12) have shown that K Monel, a copper-nickel alloy exhibits brittle delayed failure after hydrogen charging. Lai (13) and Smith (14) have given a general overview of the phenomenon of hydrogen embrittlement of nickel base alloys in recent work. Of increased importance are the studies of Walter and Chandler (15) where it has been shown that the nickel base super alloys such as Inconel 718 can be embrittled by subjecting them to a high pressure hydrogen gas environment. Further testing in this area has been carried out by Fidelle and coworkers (16). With the increasing use of hydrogen gas as a possible fuel in such areas as the space shuttle engine and in the automotive industry, these high pressure studies assume more importance and expanded work in this area will become necessary.

In addition to the characteristics of classical hydrogen embrittlement mentioned previously, the embrittlement of the nickel base alloys has several other distinctive features.

a) Serrated yielding had been observed to occur (16) which suggested that possibly mobile dislocations drag the hydrogen in (17,18). Smith (14) had observed that this could essentially be a surface effect.

b) For high concentrations of hydrogen, an unstable nickel hydride formed during the charging process. Upon removal of the charging environment, the hydride decomposed to release the hydrogen into the grain boundaries. This might then lead to grain boundary cracking (14).

c) Grain boundary embrittlement and cracking had been observed in the case of low hydrogen concentration where no visible hydriding occurred (14).

d) There seemed to be a need for small amounts of plastic deformation to initiate and continue the cracking process (10).

e) An intergranular fracture was observed (11,14,17).

f) Hydrogen was absorbed into the grain boundaries due to the presence of tin and antimony there as impurities. Tin and antimony act as hydrogen recombination poisons (17).

THE ION PROBE MASS SPECTROMETER

Within the last decade, several experimental methods have been devised which promise to give accurate microanalysis for all elements over the entire mass range. Padawer and co-workers (19) have developed a lithium nuclear microprobe which appears to yield very good results. In this method, lithium- 7 ions are accelerated to about 3 MeV and react with the hydrogen nucleus to form an excited state of beryllium. Upon returning to the ground state, gamma rays are emitted. The intensity of these gamma rays was assumed to be an indication of the hydrogen concentration for a given depth probed. There are several disadvantages with this method, however. First, it is highly specialized in that a specific nuclear reaction occur which can easily be measured. Monitoring the diffusion of any other components is not possible unless a suitable nuclear reaction occurs also. For example, the half life of the product isotope must be sufficiently long to allow for experimental measurements. This is not always possible to obtain. Second, the assumption that the energy of the gamma rays is directly related to the concentration at a given depth may not be accurate due to possible reactions occurring upon exiting and absorption of energy due to the cross-section of the sample. This problem becomes more pronounced for deeper penetrations. If these energy distributions of the product can

carefully be characterized, the method has much merit.

The laser microprobe had also been examined as a possible technique by Gray (20). In this method the laser beam heats a localized area of the sample releasing a quantity of hydrogen which is measured by the current increase in a vacuum-ion pump. There are problems in characterizing the heating process and consequently one can obtain only qualitative results.

The major experimental tool to be used in this investigation, is the ion probe mass spectrometer manufactured by the Geophysical Corporation of America. It is essentially a prototype model based on the design of Liebl. Herzog and co-workers, in several papers have described the theory and operation of this specific instrument in great depth (21,22), but some mention will be made of its operation here. The ion probe has been used in earlier work by Adler to measure hydrogen levels in titanium alloys (23). The theory of operation will be dealt with in more detail later, but briefly, an ion beam is used to sputter material from the surface of the sample. The secondary ions resulting from the bombardment are then analyzed in a mass spectrometer. This method has the advantage that there is equal sensitivity over the whole mass range and only a small quantity of material is analyzed. By varying the intensity of the bombarding ion beam, this method can be used for both surface and depth analysis. By monitoring a single species as a function of time, concentration profiles can be

measured directly as the sputtering proceeds.

A duoplasmatron is used as the primary ion source. This type of ion source was chosen for the high purity beam that is possible to obtain with it. A thoriated tungsten filament is used to emit electrons which are accelerated to the anode cup by a potential difference of approximately 85 - 110 volts. The electrons ionize very high purity argon which is bled into the chamber. To increase the electron path, the electrons are accelerated into a circular spiral to the anode by a ring of ceramic magnets which surround the entire duoplasmatron. This increases the probability that the argon gas will be ionized. All material in contact with the plasma, such as the anode cup and any apertures, is tantalum due to its availability in high purity form, its relative resistance to ion erosion and its high mass number which causes little interference in typical mass scans.

The argon ions are acclerated through a potential of 10 K.V. and focused by a series of electrostatic einzel lenses. The specimen to be analyzed is mounted at a 45° angle to the incident beam on a tantalum sample holder. No special sample preparation is necessary except that for certain applications of surface analysis, it is necessary that the surface be as clean as possible. Any type of solid may be mass analyzed except for some polymers with low vapor pressures. In the analysis of ceramic or insulator materials, a compensating filament is mounted close to the sample

to prevent excessive charge buildup during ion bombardment. The secondary ions sputtered from the surface of the sample, in addition to a portion of the primary beam which may be reflected, are then acclerated into the mass spectrometer by a second set of einzel lenses. Figure (1) shows the basic configuration of the ion source, primary optics, and secondary optics.

Mass analysis is carried out by a Mattauch-Herzog double focusing mass spectrometer. The operation of this type of mass spectrometer is described in detail by a recent paper by Herzog (24). A schematic drawing of it is given in figure (2). For this type, electrostatic and magnetostatic sectors are employed. The electrostatic field acts as an energy analyzer, while the magnetostatic sector separates the masses. An electrostatic deflection field is used to compensate for variations in energy of the ion beam. This simultaneous energy and mass separation gives rise to the term "double focusing". The double focusing configuration gives very high sensitivity and resolution over the entire mass range. In this particular instrument varying the magnetic current from 0 - 30 amps allows a mass range from 1 - 260 amu to be scanned. What is actually separated and detected is the mass to charge ratio but since the vast majority of the positive ions detected are only singly charged, it is common to refer to the scan as the mass range.

A 20 dynode electron multiplier serves as the detector and a vibrating reed electrometer measures the ion current. As the

current to the magnetic sector of the mass spectrometer is slowly increased, each mass to charge ratio is detected and the results are recorded on a X - Y recorder. The magnetic current may also be set to detect a single mass only and the behavior of this species can be monitored as a function of time.

The vacuum system of this instrument deserves some mention because it was designed to keep hydrocarbon contamination to a minimum. A six inch mercury diffusion pump is used to pump the sample chamber to a base line pressure of about 4×10^{-7} torr. A two inch mercury diffusion pump keeps the duoplasmatron evacuated. An ion pump keeps the mass spectrometer and detection sector at a vacuum of about 1×10^{-7} torr. The use of the mercury diffusion pumps and the ion pump keeps any possible hydrocarbon contamination to an absolute minimum compared with the usual oil diffusion pumps. Also, any backstreaming of the mercury which may occur, and there will always be some, will not interfere with the mass scan due to its high mass number.

The purpose of this initial work is to characterize, calibrate, and determine suitable experimental methods for the measurement of hydrogen diffusion with this type of instrument. For this purpose, samples of Monel K 500 were cathodically charged in H_2SO_4 and then sputtered to measure the diffusion of hydrogen into the sample during the charging process. An attempt was made to determine the relative amounts of hydrogen diffusing through the bulk and the grain boundary.

MATERIALS

The alloy examined in this study was Monel K 500, which is a precipitation--hardened copper-nickel alloy. The nominal composition is given in Table (1). The small amounts of aluminum and titanium precipitate as Ni_3 (Ti, Al) under a suitable age hardening treatment. Cold-rolled sheet stock of 30 mil thickness was used for examination of the fracture surface. Cold-rolled 10 mil sheet was used for the permeation samples. Prior to cathodic charging, all surfaces in contact with electrolyte were mechanically polished to a 0.5 micron surface. The polishing reduced the original sheet thicknesses approximately 4 microns. The surface was polished to insure that all surface conditions were well defined and constant.

EXPERIMENTAL PROCEDURE

Cathodic Charging

Elevated temperature cathodic charging was the method by which hydrogen had been introduced into the alloy. In this method the sample to be charged is connected to the cathode of a D.C. power supply while a platinum electrode is used as an anode. In a suitable electrolyte, the hydrogen ions are then attracted to the sample and hydrogen gas is adsorbed on the surface of the sample. Due to the high virtual pressure of the adsorbed gas, absorption or the diffusion of hydrogen occurs into the sample. The surface reactions which allow the hydrogen to be absorbed can be very complex and, as yet, little is understood as to the process that may be involved.

In all cases the charging time was a constant 24 hours and the temperature was held at 85° C by an oil bath. Temperature variation was observed to be $\pm$ 2° C. The electrolyte used was a 10 % solution of H_2SO_4. No recombination poison was used. The charging current density was the variable parameter in introducing different concentrations of hydrogen and it ranged from 500 mAmp/cm^2 to 10 mAmp/cm^2. It was desired to go to a maximum of 1 Amp/cm^2 but due to the large surface area of the samples that were necessarily employed, this was not possible. Two basic charging configurations were used.

a.) Similar to an experimental arrangement for the measurement of permeation rates, a sample was attached so that the sample was charged on one side only. The other side was open to the atmosphere. Due to the difference in hydrogen concentration on each side of the sample, a concentration gradient was induced through the thickness (26 mils). This was done over the range of current density mentioned earlier in order to see if the ion probe would be sensitive to these different levels both initially on the surface and as a function of depth into the sample.

b.) In order to attempt to differentiate between bulk and grain boundary diffusion, a different arrangement was required. In this, a specimen of the Monel K 500 was completely immersed in the electrolyte so that charging would occur more or less uniformly. These specimens were then fractured by bending in liquid nitrogen to

produce what was hoped to be essentially an intergranular fracture. The initial hydrogen level measured on the surface would then give a qualitative estimation as to the difference in hydrogen levels in the bulk and the grain boundaries.

Great pains were taken in sample handling in order to minimize both surface contamination and excessive homogenization or outgassing. Samples were transported for analysis in liquid nitrogen. When brought up to room temperature for placement into the ion probe the samples were carried in high purity freon which would leave very little residual hydrocarbon contamination on the surface. Further, this also prevented moisture condensation on the up quench. In the case of the fracture specimens, the fracturing and any cutting of the samples to size was also done in liquid nitrogen.

Ion Probe Mass Analysis

During the initial calibrations of the ion probe mass spectrometer, it was immediately obvious that, in order to compare hydrogen peak heights over a prolonged period for several different charging conditions, the main primary beam parameters had to be monitored and controlled as precisely as possible. This meant being able to reproduce primary beam conditions for each analysis. Any deviations in the conditions of the primary beam produced a corresponding variation in the detected peak height. Experimentally, high purity singly charged argon ions accelerated

to 10 K.V. were used as the primary beam. A microameter was used to monitor the ion current at the specimen and any fluctuations in the primary beam were noted here immediately. The ion beam could be focused to a spot anywhere from about 0.5 mm to 4 - 5 mm in diameter. For depth analysis of this sort, it is desirable to have as low a focus and ion current density as possible, in order to slowly and evenly remove monolayers at a time. A highly concentrated beam, although boring in faster, removes material nonuniformly producing a crater with a roughly gaussian shape.

As the sputtering continues, a sizable contribution of the secondary ions come from the sloping sides of the crater giving an erroneous concentration profile. Figures (3) and (4) show scanning electron microscope pictures of the crater bottom under light and heavy ion bombardment. Notice in figure (3) that the etching is fairly flat and uniform. Figure (4) shows the jagged cones that result from neavy or prolonged ion bombardment. It has been thought that these cones are a result of relatively sputter resistant areas essentially shielding the material under them. A practical limitation with this particular instrument lies in the fact that the filament life, operated at about 12 amps, is rather short, about 4 - 5 hours of continuous operation. Also, operation over a prolonged period may produce instrumental drift in the electronics, although this was not noted to be a serious problem. Therefore, a compromise has to be made between having

as low a current density and focus as possible and boring in at a substantial enough rate so as to produce a meaningful depth analysis. To accomplish this purpose, a medium condition of focus was chosen producing an ellipse with a minor axis diameter of about 2mm. A target current of 30 microamps was selected as a moderately low and easy to control value. As stated earlier, any primary beam variations were detected by a change in the target current measured. To compensate for any fluctuations, the filament current was adjusted accordingly. The secondary ions were accelerated across a potential of 1 KV into the mass spectrometer for analysis.

The base-line vacuum under routine conditions was 4 - 5 x 10^{-7} torr in the sample chamber and about 1x10^{-7} torr in the mass spectrometer. Bleeding argon into the duoplasmatron increases the pressure to about 1.5 - 2 x 10^{-6} torr. As a result of the fairly high vacuums obtained, the background contamination due to hydrocarbons and water vapor were noted to be very low so it would be expected that there would be a negligible contribution to the hydrogen peak from these sources.

With the instrument operating parameters thus defined, the following experimental techniques were used. To obtain a hydrogen profile, the mass spectrometer was set for the hydrogen peak manually. Adjustment for this peak is very critical since it is the sharpest of the mass peaks observed. The X-Y recorder is then used as a strip chart recorder to monitor peak height as

a function of time of sputtering. To account for any electronic drift which may occur over the period of analysis, a total mass scan of the alloy was taken before and after the analysis. In this case any possible drift can be noted by observing the behavior of the main matrix element, in this case, nickel. The hydrogen scan can then be normalized with respect to the nickel by assuming a linear drift in the nickel peak. The ideal method is to have the ability to continuously monitor several preset peaks simultaneously, but this feature was not available on this instrument. All the hydrogen profile data will then be presented as ratios with respect to nickel. The procedure used was to bombard an area to obtain the initial mass scan. The beam was then shut off and the sample translated so that the beam would strike a fresh area. Here then, for a period of about 3000 - 5000 seconds, the hydrogen peak was monitored until it became evident that the gradient was fairly constant. The final mass spectrum scan was then taken on this area after the analysis was terminated. Much the same technique was employed to examine the fracture surfaces, although initial adjustments were much more critical since the first several seconds of sputtering would give the hydrogen level in the grain boundaries. The boundaries would be sputtered through quite rapidly, and after that, only bulk levels would then be noted.

RESULTS

A mass scan of the Monel K 500 is given in figure (5) with the major species identified. The high sensitivity to easily ionized surface contaminants such as sodium and potassium is illustrated but very little carbon or water had been noted in routine analysis, indicating little background from these sources.

A sputtering rate was estimated by sputtering for a fixed period of time on a polished surface. A scanning electron microscope was then used to take a stereo photomicrograph of the crater. The method used to determine the crater depth is given in appendix A. Best estimations of the sputtering rate yield a value of approximately 7 microns per hour. Using this value for the rate, the concentration-time profiles may be converted to concentration-depth profiles. Variations of the primary beam conditions, of course, lead to different sputtering rates. For this reason, the primary beam conditions were kept constant for each experiment. Furthermore, this rate would not be the same if a different material had been used so that this rate refers to a highly specific condition.

The hydrogen profiles of the permeation specimens as a function of the charging current density are given in figure (6). Several features can be noted.

a) Increasing the charging current density increased the amount of hydrogen pickup.

b) There is a somewhat higher concentration of hydrogen on the surface of the samples. This concentration rapidly falls off as the sputtering proceeds. These high surface concentrations of hydrogen resulting from cathodic charging have been observed by a number of earlier workers (31) for iron and nickel wires. In the case of nickel, the higher surface concentrations have been attributed to an unstable hydride layer, but this has been difficult to verify in this study due to the overlap of many mass peaks in this region. According to Latanision (17), this surface hydrogen is then dragged inward by mobile dislocations resulting from Frank-Read sources near the surface.

c) The uncharged sample had a very low residual hydrogen level ($I_H+/I_{Ni}+ = 0.0035$). Originally, it was thought necessary to subtract out the background level in order to measure the amount of hydrogen which had been absorbed in the charging process. Substantial hydrogen pickup by the charging allowed the background to be considered negligible.

c) A cross over in the penetration curves is noted for 100 mAmp/cm^2 and 10 mAmp/cm^2 after sputtering for about an hour. The concentrations for these charging current densities are fairly close over a wide range of sputtering times. In a reproduction of several runs, a reasonable error bar in the detected intensity is 0.1. It is not

yet known why the curves cross or why the detected concentrations are very nearly equal for the two charging conditions. Experimental error makes it difficult to draw any positive conclusions.

The initial hydrogen concentration on the surface is presented as a function of the charging current density in figure (7). This curve is qualitatively similar to a Sievert's law plot. Bodenstein (25), in early work, demonstrated that the permeation of hydrogen in steel was related to the charging current density in a like manner.

$$P = ki^{1/2}$$

where P = Permeation
k = constant
i = charging current density

Assuming $I_H+/I_{Ni}+$ is proportional to the permeation, the constant (k) is calculated in Table (2) for each data point. It can be seen that the constants are fairly close in value indicating that the above relationship may be valid. With time, however, as the sample heats up, homogenization of the hydrogen gradient and outgassing may be expected to occur to some extent.

In order to predict hydrogen levels at deeper penetrations, the gradients were then calculated for times greater than about 100 sec. which allow for surface effects to be ignored. The results are presented here. The units for concentration (peak intensity) are arbitrary.

a) For 500 mAmp/cm^2, $\Delta C/\Delta x$ = -0.0156/ micron

b) For 100 mAmp/cm^2, $\Delta C/\Delta x$ = -0.0052/ micron

c) For 10 mAmp/cm^2, $\Delta C/\Delta x$ = -0.0025/ micron

It should be noted that these measured gradients approximately follow the $i^{1/2}$ dependence mentioned earlier.

Samples were then charged and fractured in liquid nitrogen in an effort to produce an intergranular fracture to examine hydrogen concentrations in the grain boundaries. Previous work by Papp (11) on the cathodic charging of Monel K 500 indicated that a completely intergranular fracture could be obtained. Figures (8) and (9) indicate, in this case that the fracture mode appeared to be mixed. Light micrography, figure (10) indicated a relatively uniform grain size in a section transverse to the rolling direction. Overall examination of the fracture surface indicated that, on the tension side of the bend, the fracture mode was predominantly one of cleavage with some ductile failure. On the other hand, failure on the compression side was completely ductile. Evidence of the intergranular cracking reported by Smith (14) and Latanision (17) was not observed. However, alloys used were probably equiaxed. In the distorted structure studied here, it is possible that the secondary cracking observed in Figure (8) is at least partly intergranular. Also, comparison of the grain size in Figure (10) with the average feature size and range in the fractograph in Figure (9) shows a correspondence. Therefore, although features typical of an equiaxed intergranular fracture are not obvious, it is

reasonable to assume that a higher proportion of grain boundary area was present on the fracture surface.

Figure (11) shows the hydrogen profile on the fracture surface. It was not possible to charge a sample to 500 mA/cm^2 because of the large surface area of these samples, but the results of the other two charging conditions correlate well. It is evident that a much higher hydrogen level was detected here than for the surface (bulk) sputtering of the permeation sample in each case. The increase in each case was approximately an order of magnitude. Furthermore, as would be expected, while the initial levels were much higher, the concentration fell off very rapidly as the sputtering progressed to bulk levels, which approximately correspond to the bulk levels of the permeation samples. It would not take very long to erode the grain boundary surface so the rapid fall off was expected. Furthermore, the time taken for the fall off (less than 10 seconds) corresponds roughly to a grain boundary thickness using the estimated sputtering rate. Also, a possible contribution to the higher hydrogen levels detected here may be due to the higher surface area of the fracture. Had the fracture been more of an intergranular nature, it might have been possible to measure the relative proportion of hydrogen in the bulk and the grain boundaries.

In order to determine whether or not the higher concentration detected on the fracture surface was due to adsorbed hydrogen picked up in the charging process or due to hydrocarbon contamination, further experimentation was carried out. A sample was charged at a current density of 100 mAmps/cm^2 under identical charging conditions as the other samples. In this case, however, a mass scan was made of the carbon peak instead of the hydrogen. No corresponding high level of carbon was noted at the surface. The gradient was rather level, and, in fact, increased slightly at greater depths. This was probably due to the carbon which exists as a tramp element in the alloy.

The presence of tin and antimony, which are hydrogen recombination poisons (16) was difficult to observe in the mass scan of the fracture surface. Occurring only in minute quantities in the grain boundaries, their mass peaks would not be large. Furthermore, in this mass range, the background is usually somewhat higher and would therefore obscure these peaks. Suppressing the background still does little to positively confirm the existance of these elements. While therefore, it is possible that these elements are present, there is no conclusive proof as to either the quantity or location of these elements.

There were two inherent experimental problems that were noted, but unfortunately could not be eliminated. Since it was

vital that the background contamination levels be as low as possible, it was necessary to work under high vacuum conditions. It would then be expected that some outgassing may occur. To what extent the sample outgassed is not known and is difficult to determine with this instrument since the gas would be neutral. According to Gray and co-workers (26), though, there is reason to believe that outgassing does not occur rapidly in the nickel based alloy. In the appendix (B), a calculation was made of the degree of outgassing that might be expected under these experimental conditions. It was observed, that for the times of analysis used here that the outgassing would not be excessive.

A second experimental difficulty which was expected was that of sample heating during ion bombardment. The use of a cold stage would solve this difficulty although a major modification of the instrument would be necessary. The use of a relatively large mass sample holder and the use of small thin samples minimize this problem by employing heat transfer. In order to monitor specimen heat up with time, an iron-constantan thermocouple was spot welded to a dummy sample of the Monel K 500. The results are given in figure (12). It is observed that most of the heating occurs in the first 10 - 15 minutes and there is a leveling off and a very slow increase after 30 minutes. It is not expected, then, that over the times required for analysis the sample heats up much over 45 - 50^{o} C which was a surprisingly low value.

As stated before, although a cold stage would be the ideal experimental set up, the heating was much less severe than originally expected and is not considered to be a major problem.

SUGGESTIONS FOR IMPROVEMENT

In establishing a workable experimental procedure, several instrument shortcomings were noted. Since the GCA instrument was essentially a prototype model and was not meant for general production, many conveniences were not added. Most of the following suggestions for modifications are in the primary beam and stage area. The mass spectrometer and detection system operated very well.

Suggestions for improvements are:

a) Use an alternate ion source that would be stable over extended periods of operation. The duoplasmatron, while given a high purity, stable and homogeneous beam for short periods is limited by the life of the filament which can be very short because of the high current needed for adequate emission. A cold cathode ion source is the type usually employed for this type of application. This source can be operated for much longer periods of time, since a very low current density beam is used. As noted earlier, the advantage of a low current density beam is a slower and more uniform material removal rate to give more sensitive results. Cratering does not occur so that an accurate removal rate can be determined. An added advantage, also would be less sample heat up, although, as determined in this study, that heat up is not overly large.

b) Modify the einzel lens system in the primary beam

system to reduce the beam size to microprobe proportions. A low current density defocused beam is roughly 5 - 6 mm in diameter. This large beam size makes it impossible to focus on highly localized areas of the sample.

c) In keeping with (b), a smaller beam size necessitates the use of an adequate optical system for focusing on the desired area of the sample. In the present system, only several viewing ports are available. A series of tantalum shields can be used to keep the sputtering highly localized when necessary, but accurate positioning of these shields is difficult.

d) Provision should be made for a cold stage to minimize outgassing and homogenization that may occur over extended analysis periods. Also, to provide for some flexibility, certain experiments may necessitate the use of a hot stage as well. Provisions should be made for this also.

e) Allow for the monitoring of several preset elements simultaneously. In this way, the nickel peak could be monitored at the same time as the hydrogen and no assumptions would have to be made as to any possible instrumental drift. It is not known as yet whether or not this modification can be made to a double-focusing mass spectrometer. This multi-element scan has already been employed in quadruple mass spectrometers, so it seems reasonable to assume that it could be used here also.

While it was easy to recognize the shortcomings of this

particular instrument, any of the above suggestions would require extensive modification.

Of the suggestions listed here, a), c), and e) could be practically carried out and an attempt will be made to do so for future work. Newer commercial models have employed not only these, but other refinements, such as a scanning system to give an ion picture of the desired species.

SUMMARY AND CONCLUSIONS

1) The ion probe mass spectrometer is very sensitive in the detection of hydrogen, making it a potentially valuable tool to evaluate hydrogen embrittlement mechanisms.
2) All operating parameters in the instrument must be recognized and controlled in order to compare results from analysis to analysis.
3) Major difficulties with the instrument are the lack of spatial and depth resolution and the inability to employ long term analysis. These difficulties can be alleviated by modifications to the existing design.
4) Surface and depth analysis can be carried out in a routine procedure in order to obtain relative concentrations of the species of interest.
5) While no attempt was made to quantitatively interpret the results here for the hydrogen diffusion in the Monel K 500, most of the qualitative results were reasonable.
6) Evidence is presented here to support the theories of previous workers that there is a substantially higher concentration of hydrogen in the grain boundaries of the monel than in the bulk.

BIBLIOGRAPHY

1. Fast, J.D., Introduction of Metals and Gases, Academic Press, New York, 1965, Ch. 7.

2. Troiano, A.R., Trans. ASM, Vol. 52, 1960, pp. 54.

3. Zapffe, C.A. and Sims, C.E., Metals and Alloys, Vol. 11, 1940, pp. 145.

4. Tetelman, A.S., Hydrogen in Metals, Seven Springs, Pa., Sept., 1973, pp. 17.

5. Gest, R.J. and Troiano, A.R., "L' Hydrogene dans les Metaux", Editions Science et Industrie, Paris, May, 1972, pp.427.

6. Whiteman, M.B. and Troiano, A.R., Corrosion, Vol. 21 1965, pp. 125.

7. Boniszewski, T. and Smith, G.C., Acta Met., Vol. 11, 1965, pp. 165.

8. Wilcox, B.A. and Smith, G.C., Acta Met., Vol. 13, 1965, pp. 331.

9. Mihelic, J.L., PhD. Thesis, Case Institute of Technology, 1964.

10. Mihelic, J.L. and Troiano, A.R., Nature, Vol. 197, 1963, pp. 996.

11. Papp, J., PhD. Thesis, Case-Western Reserve University, 1974.

12. Papp, J., Hehemann, R.F., and Troiano, A.R., Hydrogen in Metals, Seven Springs, Pa., Sept., 1973, pp. 657.

13. Lai, G.Y., PhD. Thesis, North Carolina State University, 1972.

14. Smith, G.C, Hydrogen in Metals, Seven Springs, Pa., Sept., 1973, pp. 485.

15. Walter, R.J. and Chandler, W.T., Hydrogen in Metals, Seven Springs, Pa., Sept., 1973, pp. 515.

16. Fidelle, J.P., "Quick Pressure Hydrogen Embrittlement Test of Metal Disks", Colloquium, Hydrogen in Metals, Valduc, edited by Le Centre d'Etudes de Bruyeres-le-Chatel, 91 France, Sept., 1967, pp. 131.

17. Latanision, R.M. and Opperhauser, H., Met. Trans., Vol. 5, 1974, pp. 483.

18. Fidelle, J.P., Discussion to paper by R.M. Latanision: Corrosion Fatigue, N.A.C.E., Houston, 1972, pp. 185.

19. Padawer, G.M. and Adler, P.N., "Development of a Nuclear Microprobe Technique for Hydrogen Analysis in Selected Materials", Final Report, Grumman Aerospace Corporation, 1973.

20. Gray, H.R., Corrosion, Vol. 28, 1972, pp. 47.

21. Barrington, A.E,, Herzog, R.F.K., and Poschenrieder, W.P., "The Ion Microprobe Mass Spectrometer", Progress in Nuclear Energy, Series IX, Vol. 7, Pergamon Press, New York, 1966.

22. Herzog, R.F.K., Poschenrieder, W.P., and Satkiewicz, F.G., N.A.S.A. Contractor Report CR-683, Goddard Space Flight Center, 1967.

23. Adler, P. and Kennedy, J., Grumman Research Memorandum RM-545, Grumman Aerospace Corporation, 1972.

24. Herzog, R.F.K., "The Transmission of Ions through Double Focusing Mass Spectrometers", Trace Analysis by Mass Spectrometry, Academic Press, New York, 1972, pp. 57.

25. Fletcher, E.E. and Elsea, A.R., Defense Metals Information Center Report 219, Battelle Memorial Institute, June, 1965.

26. Gray, H., "The Embrittlement of Ni, Co, and Fe Based Superalloys by Hydrogen," Report D-7805, National Aeronautics and Space Administration, 1974.

27. Boyde, A., Proceedings of the Third Annual Scanning Electron Microscopy Symposium, Chicago, 1970, pp. 107.

28. Anderson, C.A., Colby, J., and Dobrott, R., Pittsburg Conference on Analytical Chemistry and Applied Spectroscopy, Cleveland, March, 1974.

29. Carslaw, H.S. and Jaeger, J.C., Conduction of Heat in Solids, Second Edition, Oxford Press, London, 1959.

30. Hill, M.L. and Johnson, E.W., Acta Met. Vol. 3, 1955, pp. 566.

31. Smialowski, M., Hydrogen in Steel, Pergamon Press, London, 1962, pp. 49.

APPENDIX A

SPUTTER RATE DETERMINATION

In order to obtain any meaningful information as to the hydrogen penetration into the Monel K 500, the sputtering or erosion rate must be determined for a given set of experimental conditions. This converts the concentration-time into concentration-distance profiles, assuming a uniform rate of erosion. There are several ways by which this can be accomplished. The method employed in this study was to mechanically polish a sample and sputter it for a given amount of time. Stereo pair photographs were taken in a scanning electron microscope by using a tilt only method. This technique is described in more detail by Boyde (27). For the tilt only method the depth (Z) may be calculated from the relationship:

$$Z = \frac{P}{2} \operatorname{Sin} \frac{\alpha}{2}$$

where P = Parallax which is defined as $|d_2 - d_1|$, the difference in the distance between any corresponding points normal to the tilt axis and α = tilt angle. There is some error involved at low magnifications so it is desirable to use as high a magnification as possible. Initial calculations yielded a depth on the order of 1 - 2 microns after an hour of sputtering. As seen in figure (4) however, sizable spikes are observed at higher magnification which are estimated to be on

the order of 7 - 10 microns in height. It is reasonable to assume then that the 1 - 2 micron value is the depth measured from the datum plane to the top of these spikes, but the actual erosion occurs to a greater depth. The problem as to what statistically constitutes the representative depth of analysis is then very difficult and is one subject of intensive research by C. A. Andersen and co-workers (28). A reasonable estimate as to the mean rate might be about 7 microns per hour under the experimental conditions employed here. The data will be presented, though as a function of sputtering time. This rate should give a fair indication as to the depth of penetration at any given time by a simple conversion.

APPENDIX B

ANALYSIS OF THE OUTGASSING OF A THIN SLAB WITH A LINEAR CONCENTRATION GRADIENT

Consider a thin slab of thickness (l) with, initially, a linear concentration gradient through it. Furthermore, this slab is to be contained in a vacuum. In this case, Fick's second law must be solved in order to obtain an expression for the concentration of the diffusing species as a function of depth and time. Details of the solution may be found in Carslaw and Jaeger (29). Fick's second law is given as

$$\frac{\partial C}{\partial t} = D \frac{\partial^2 C}{\partial x^2}$$

for $0 < x < 1$

where C = Concentration of the diffusing species

D = Diffusivity

t = Time

x = Distance into the slab

This equation must be solved for the boundary conditions

$$C = 0 \quad \text{when} \quad x = 0 \quad \text{and} \quad x = 1$$

and

$$C = f(x) \quad \text{when} \quad t = 0$$

In this case, assuming an initial linear gradient through the slab,

$$f(x) = kx$$

where k = Constant of proportionality.

Using a sine series solution for Fick's second law and for the given boundary conditions, one obtains

$$C(x, t) = \frac{2kl}{\pi} \sum_{n=1}^{\infty} \frac{(-1)^{n-1}}{n} \exp(-Dn^2\pi^2 t/l^2) \sin \frac{n\pi x}{l}$$

Let $$C_o = kl$$

and plot

$$\frac{C(x, t)}{C_o} \quad \frac{2}{\pi} \sum_{n=1}^{\infty} \frac{(-1)^{n-1}}{n} \exp(-Dn^2\pi^2 t/l^2) \sin \frac{n\pi x}{l}$$

From the work of Hill and Johnson, $D \simeq 3 \times 10^{-9}$ cm^2/sec for T = 300°K. The approximate value of (l) used was 6 mils, the thickness of the permeation samples used in this study. For the sake of convenience the first three terms of the infinite series are plotted only. The results are given in figure (13).

As can be seen, outgassing does not proceed rapidly until the time exceeds about 5×10^3 seconds. About halfway through the thickness, however, the gradient is not altered. Approximate time of analysis plus the pump down time usually did not exceed 5×10^3 seconds.

It is to be emphasized, though, that the outgassing behavior predicted here is the result of several simplifying assumptions.

The slab is assumed to be homogeneous with no short circuit diffusion paths such as grain boundaries or dislocation pipes. No trapping at voids is considered and all the hydrogen is assumed to be in a diffusible monatomic form at all times. Also, any adsorbed hydrogen on the surface is neglected. For the times of analysis used in these experiments, the ideal outgassing behavior does not seem to put serious limitations on the interpretation of the experimental hydrogen concentration profiles measured here. For more accurate data reduction, the outgassing effect can be superimposed to correct the measured profiles, but this should be necessary for long term analysis only. For measurements of the surface effects outgassing may be neglected.

NICKEL (PLUS COBALT)	63.0-70.0
CARBON	0.25 MAX.
MANGANESE	1.50 MAX.
IRON	2.00 MAX.
SULFUR	0.01 MAX.
SILICON	0.50 MAX.
COPPER	BALANCE
ALUMINUM	2.30-3.15
TITANIUM	0.35-0.85

TABLE 1. Composition of Monel K 500 in weight percent

i (mAmp/cm^2)	P (I_{H^+}/I_{Ni^+})	P^2	$k=P^2/i$
10	0.167	0.028	0.0028
100	0.670	0.450	0.0045
500	1.500	2.250	0.0045

TABLE 2. Curve fit of Sievert's law to initial hydrogen levels

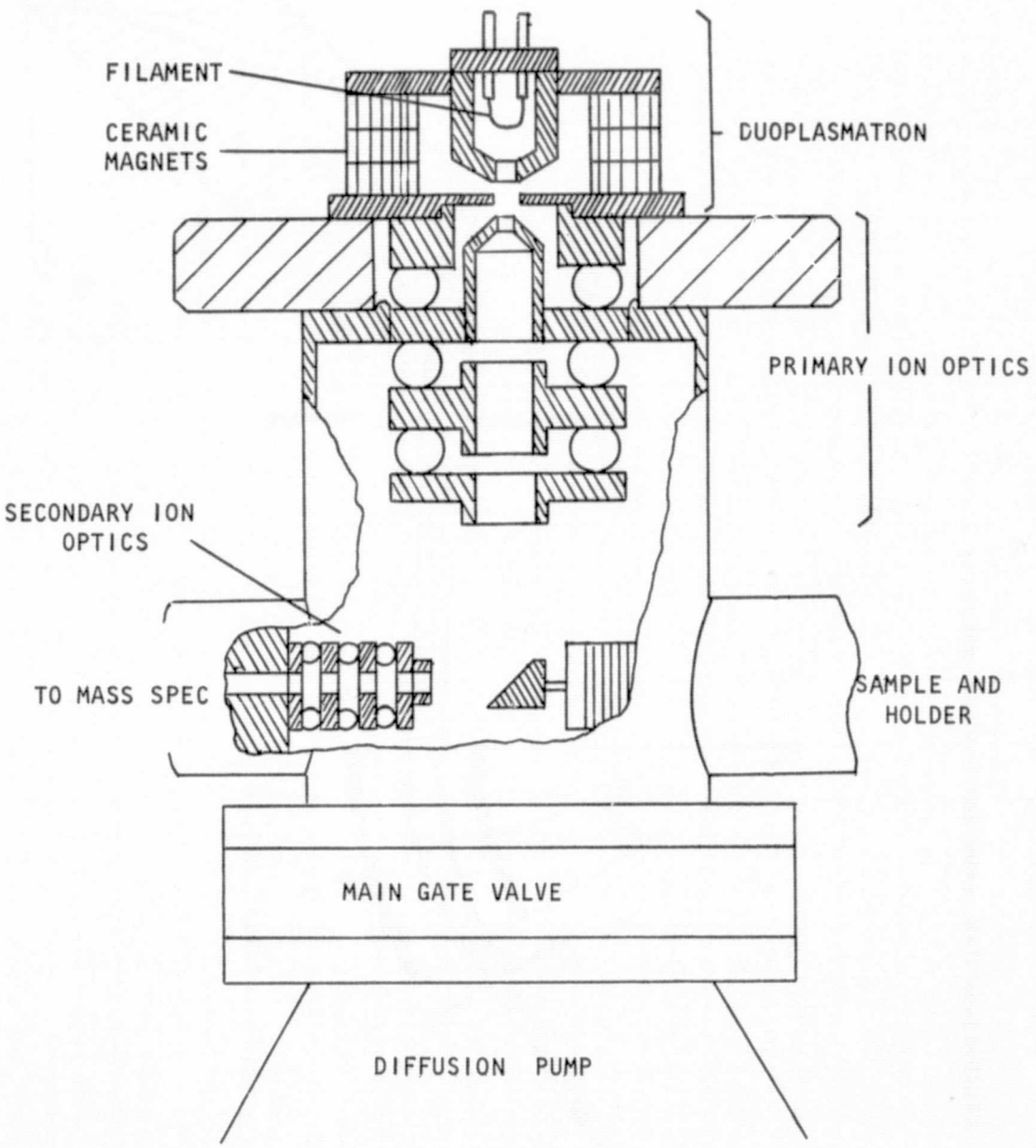

FIGURE 1. Ion source, primary and secondary ion optics.

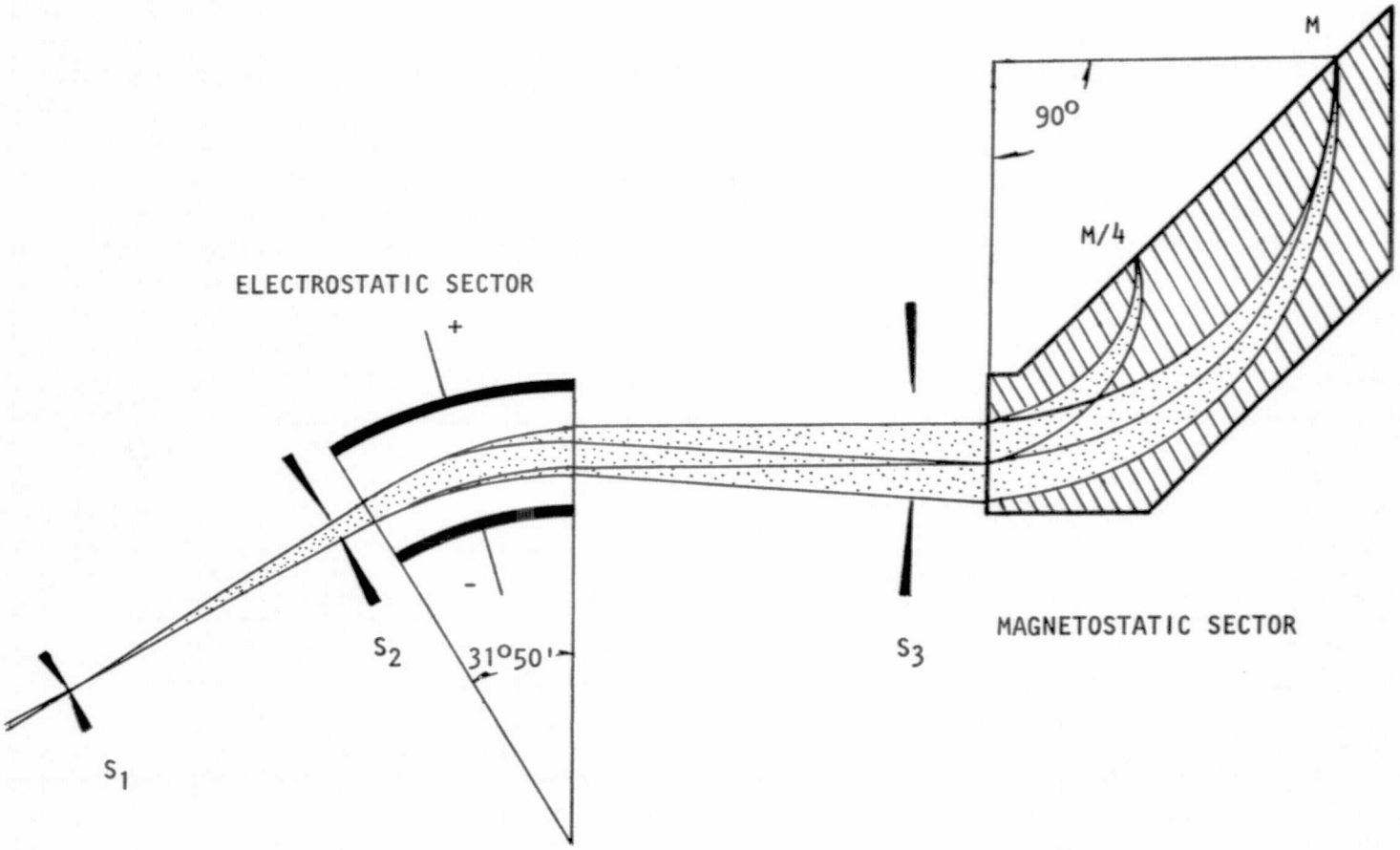

FIGURE 2. Mattauch-Herzog type mass spectrometer

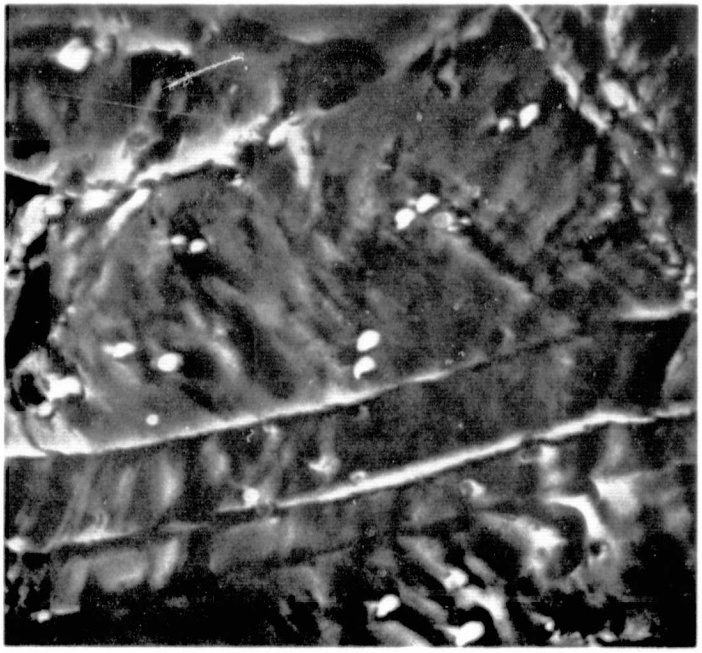

FIGURE 3. Surface of Monel K 500 after light ion bombardment. 3000x.

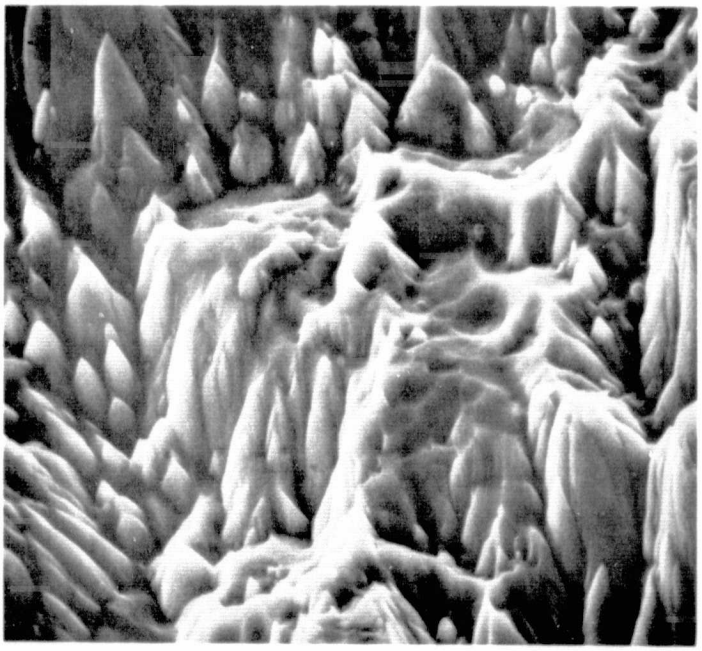

FIGURE 4. Surface of Monel K 500 after heavy ion bombardment. 3000x.

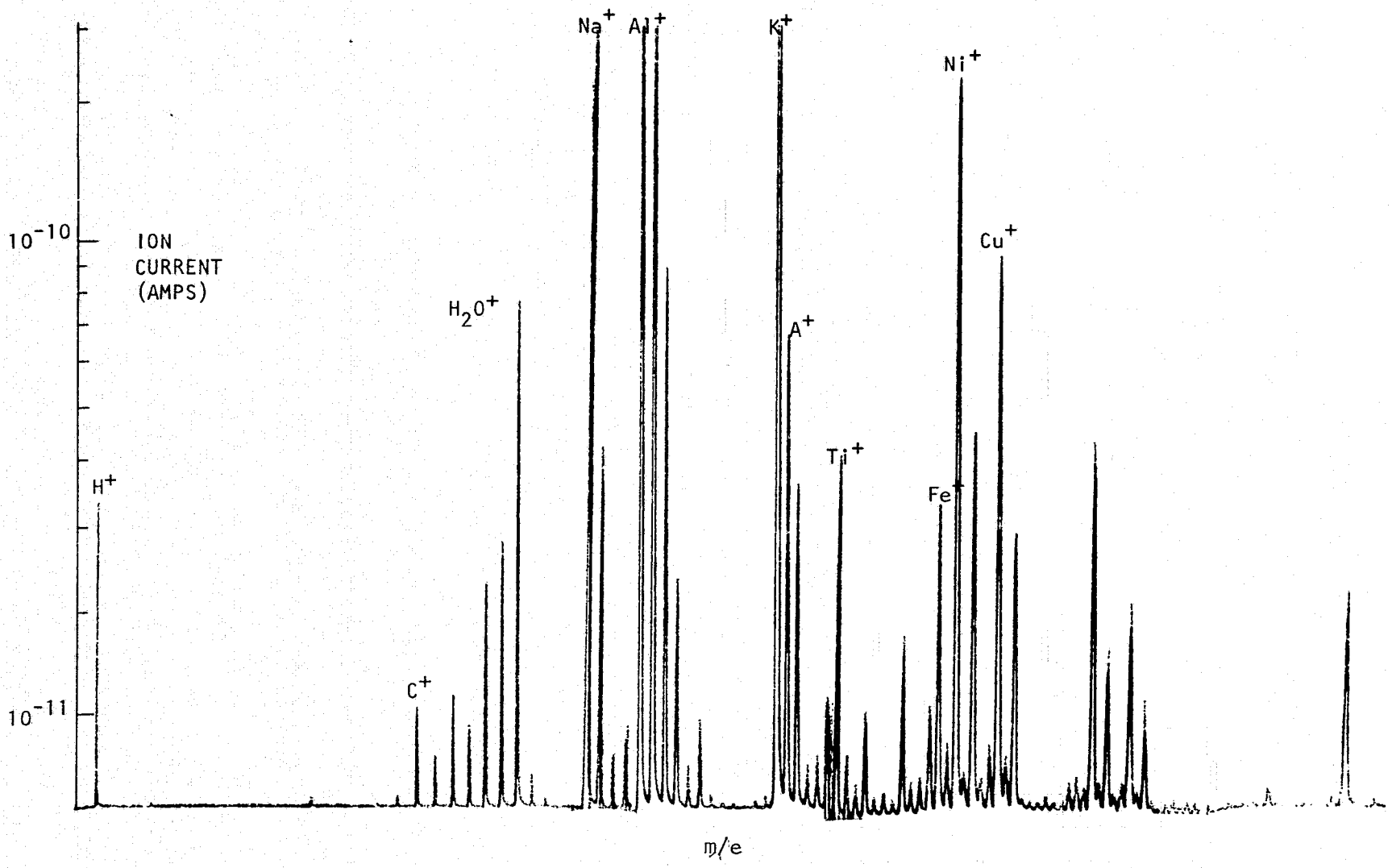

FIGURE 5. Mass scan of Monel K 500 showing major alloy components.

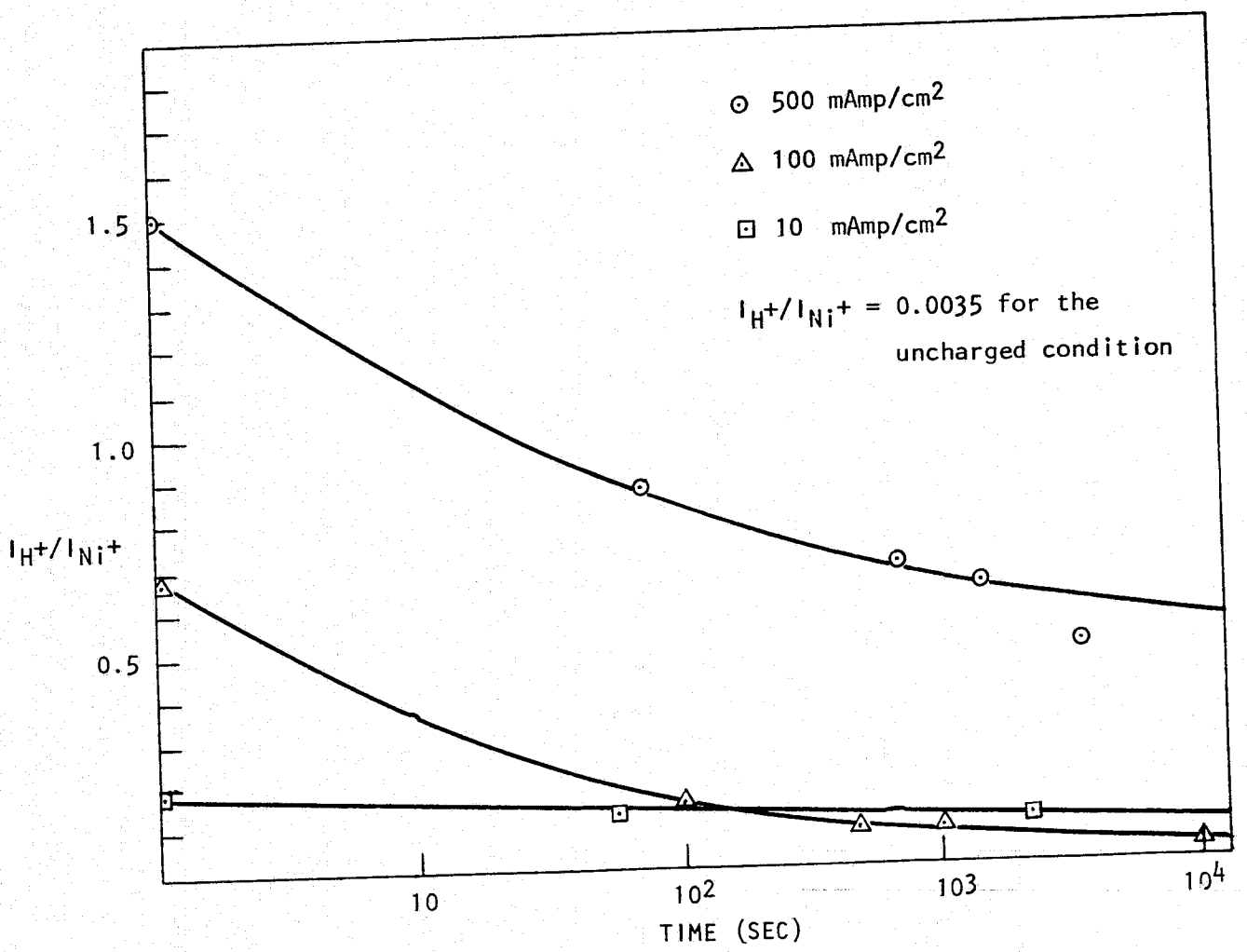

FIGURE 6. Hydrogen profiles of the permeation specimens

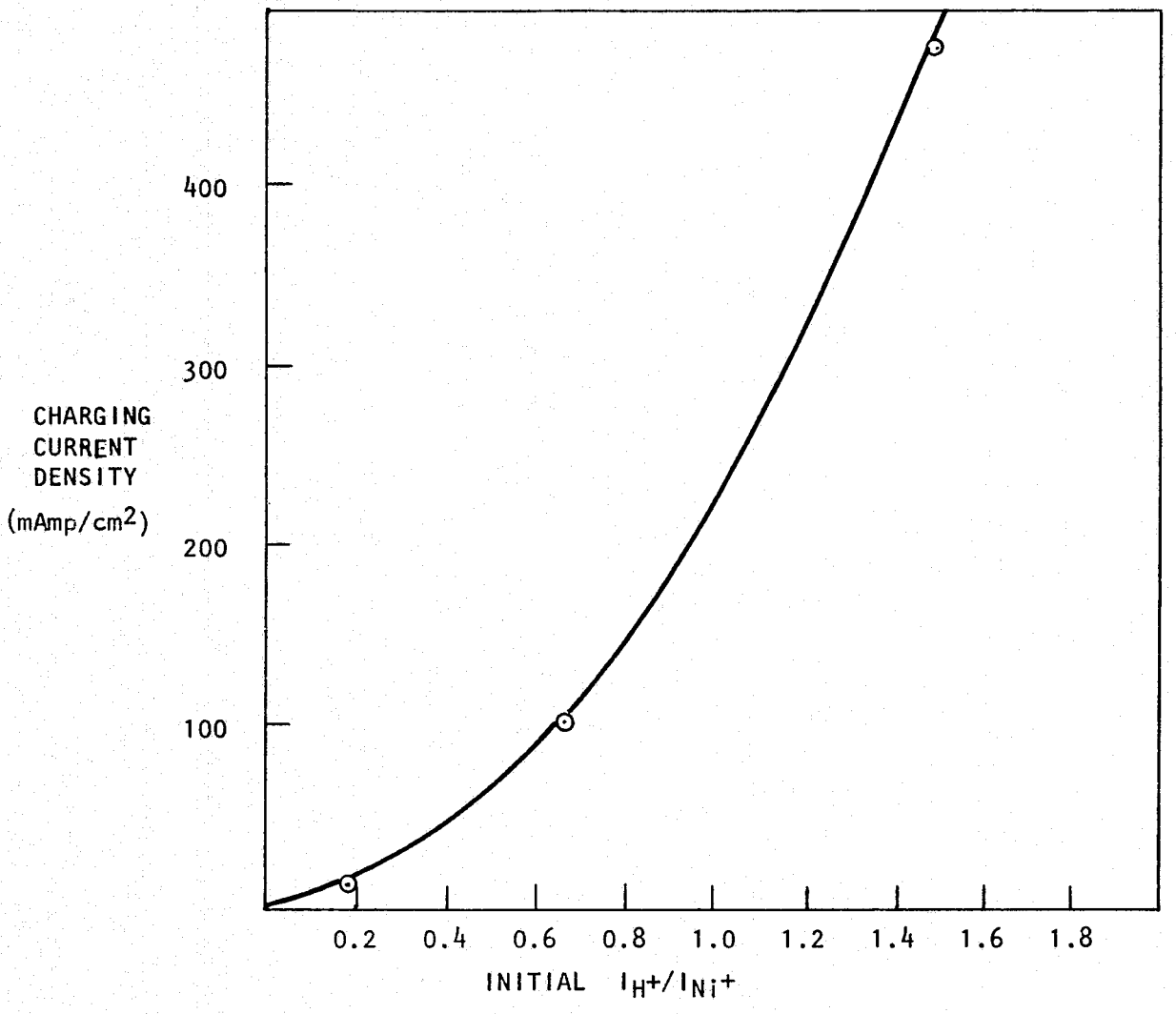

FIGURE 7. Initial hydrogen concentrations as a function of charging current density

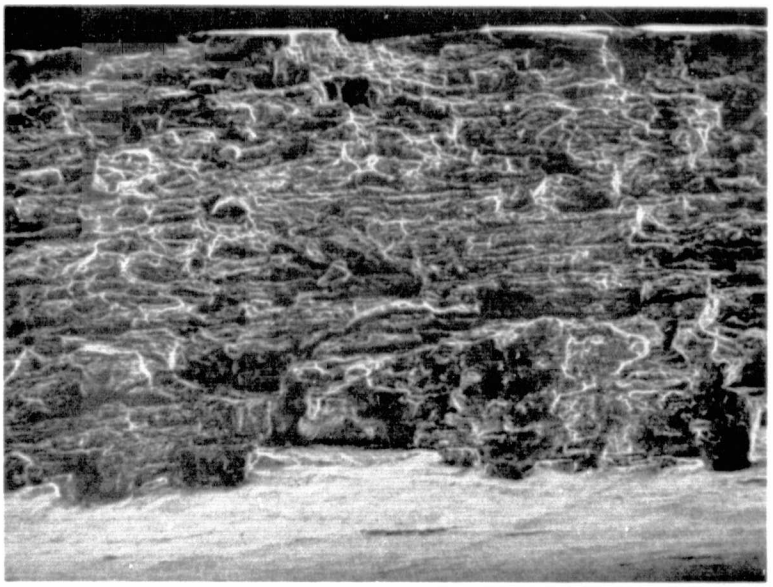

Figure 8. Surface of the hydrogen charged Monel K 500 fractured in bending. Lower edge is tension side of the bend. 100 x.

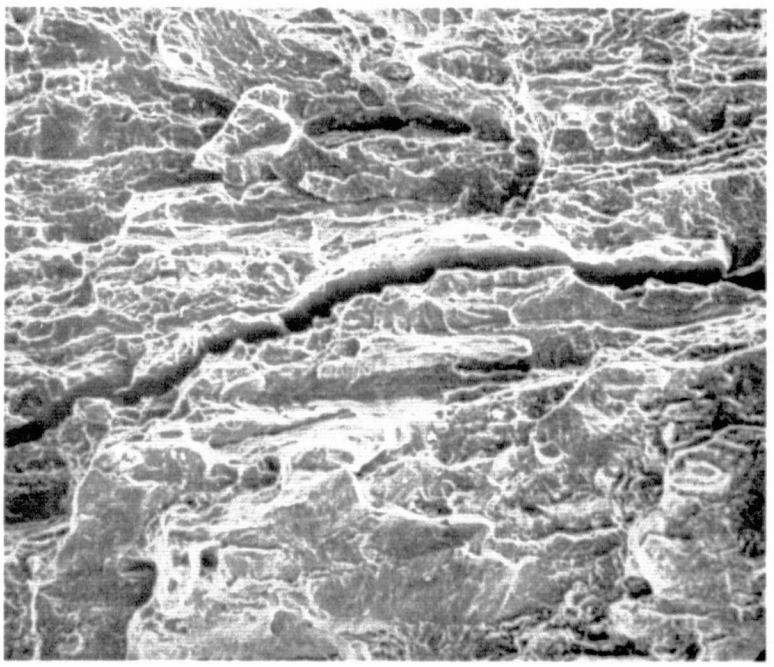

Figure 9. Detail of cleavage and secondary cracking on the fracture surface. 300 x.

FIGURE 10. Microstructure of Monel K 500. Section taken is transverse to the rolling direction. 250x.

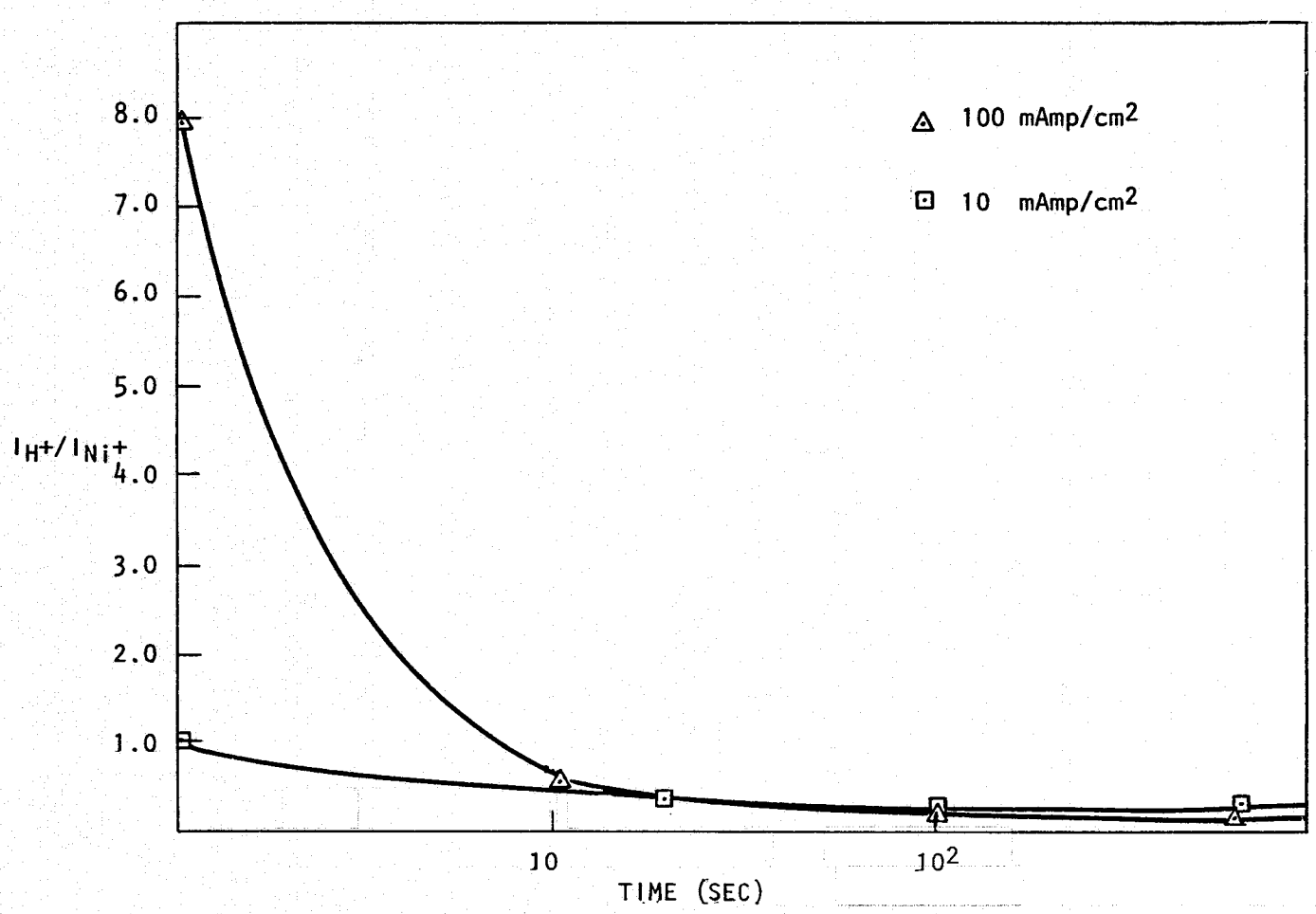

FIGURE 11. Hydrogen profiles of the fracture surface

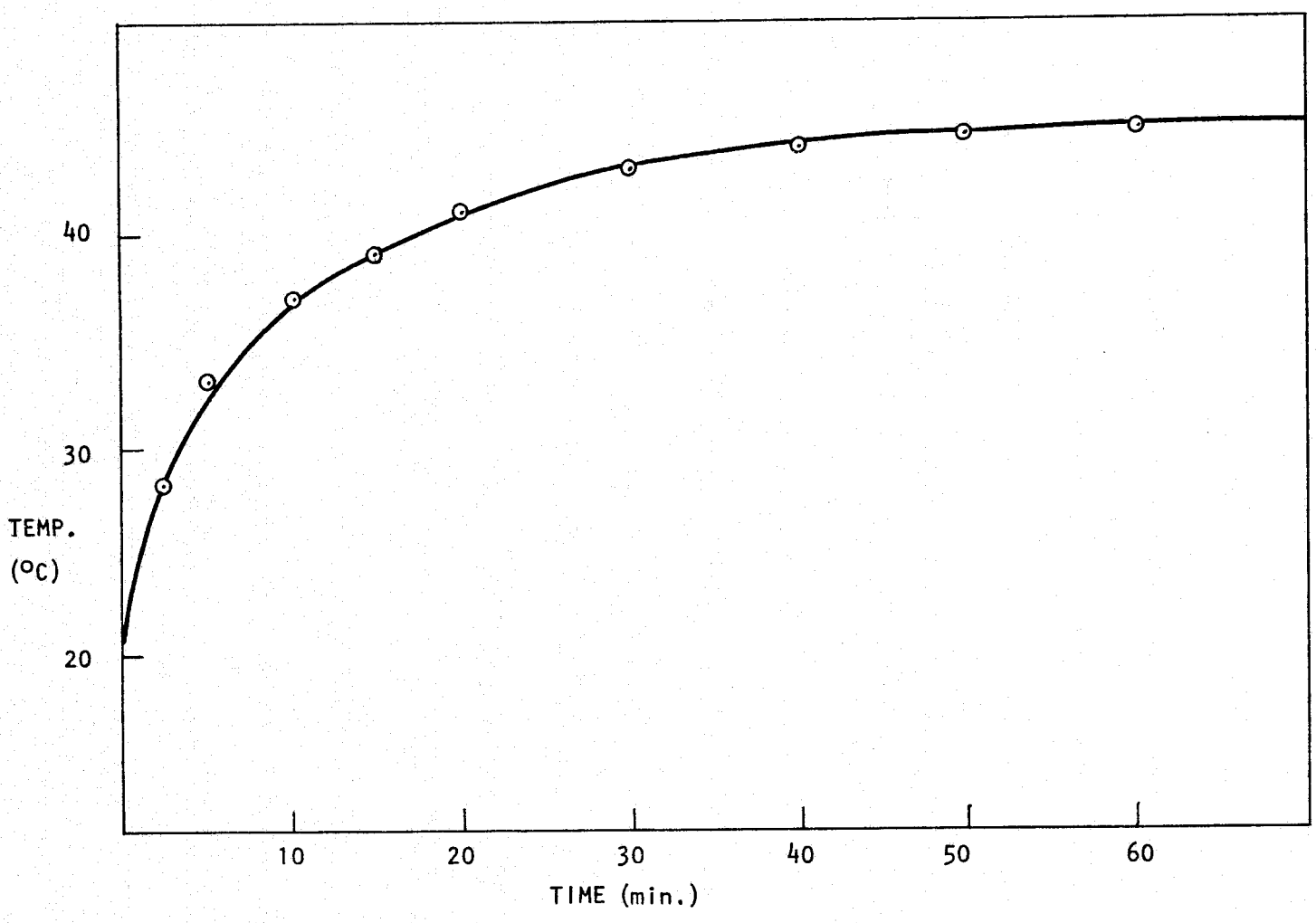

FIGURE 12. Temperature buildup in the Monel K 500 during ion bombardment

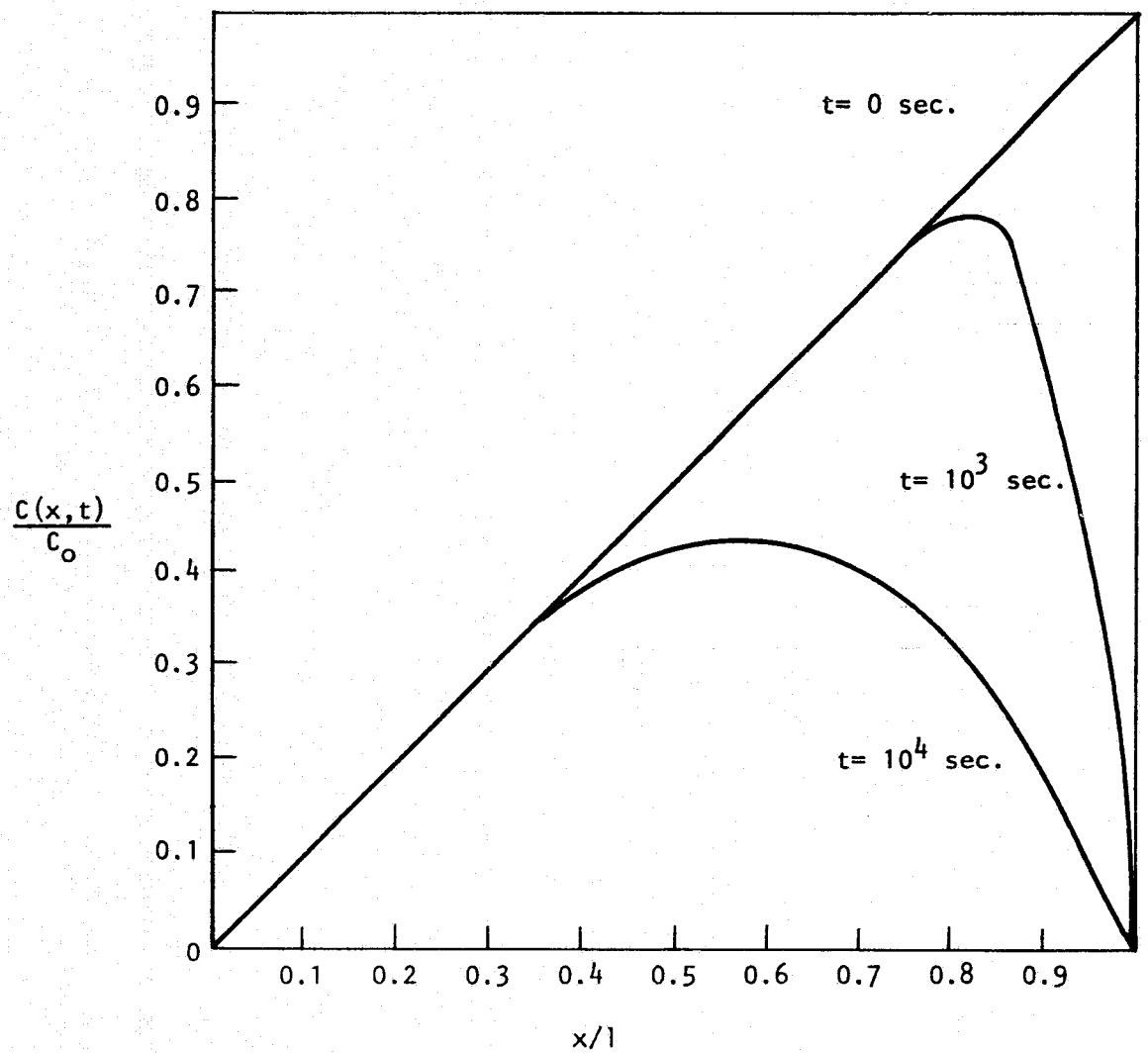

FIGURE 13. Calculated hydrogen concentration gradients in Monel K 500 as a function of time